BIOCHEMICAL PHARMACOLOGY 77 (2009) 348–363

available at www.sciencedirect.com

ScienceDirect

journal homepage: www.elsevier.com/locate/biochempharm

Novel derivatives of spirohydantoin induce growth inhibition followed by apoptosis in leukemia cells

Kavitha C.V.[a], *Mridula Nambiar*[a], *Ananda Kumar C.S.*[b], *Bibha Choudhary*[c], *Muniyappa K.*[a], *Kanchugarakoppal S. Rangappa*[b,**], *Sathees C. Raghavan*[a,*]

[a] *Department of Biochemistry, Indian Institute of Science, Bangalore 560012, India*
[b] *Department of Studies in Chemistry, Manasagangotri, University of Mysore, Mysore 570006, India*
[c] *Manipal Institute of Regenerative Medicine, Manipal University, Bangalore 560071, India*

ARTICLE INFO

Article history:
Received 13 August 2008
Accepted 16 October 2008

Keywords:
Chemotherapy
Double-strand break
Cytotoxicity
Cell death
Anticancer drugs
Flow cytometry
DNA damage

ABSTRACT

Hydantoin derivatives possess a variety of biochemical and pharmacological properties and consequently are used to treat many human diseases. However, there are only few studies focusing on their potential as cancer therapeutic agents. In the present study, we have examined anticancer properties of two novel spirohydantoin compounds, 8-(3,4-difluorobenzyl)-1′-(pent-4-enyl)-8-azaspiro[bicyclo[3.2.1] octane-3,4′-imidazolidine]-2′,5′-dione (DFH) and 8-(3,4-dichlorobenzyl)-1′-(pent-4-enyl)-8-azaspiro[bicyclo[3.2.1]octane-3,4′-imidazolidine]-2′,5′-dione (DCH). Both the compounds exhibited dose- and time-dependent cytotoxic effect on human leukemic cell lines, K562, Reh, CEM and 8E5. Incorporation of tritiated thymidine ([^{3}H] thymidine) in conjunction with cell cycle analysis suggested that DFH and DCH inhibited the growth of leukemic cells. Downregulation of PCNA and p-histone H3 further confirm that the growth inhibition could be at the level of DNA replication. Flow cytometric analysis indicated the accumulation of cells at subG1 phase suggesting induction of apoptosis, which was further confirmed and quantified both by fluorescence-activated cell sorting (FACS) and confocal microscopy following annexin V-FITC/propidium iodide (PI) staining. Mechanistically, our data support the induction of apoptosis by activation of the mitochondrial pathway. Results supporting such a model include, elevated levels of p53, and BAD, decreased level of BCL2, activation and cleavage of caspase 9, activation of procaspase 3, poly (ADP-ribosyl) polymerase (PARP) cleavage, downregulation of Ku70, Ku80 and DNA fragmentation. Based on these results we discuss the mechanism of apoptosis induced by DFH and its implications in leukemia therapy.

1. Introduction

Cancer has been proven to be a difficult disease to cure and few effective drugs are available. The development of novel, efficient, selective, and less toxic anticancer agents remains an important and challenging goal in medicinal chemistry. Hence, understanding the molecular mechanism involved in cancers will lead to novel ways in the development of new anticancer agents. Changes in DNA, RNA and protein levels as a result of mutations have been analyzed in many cancers, including leukemia and lymphoma [1–4]. Recently, there have been extensive efforts towards characterization of the mechanism of chromosomal translocations and deletions in many leukemia and lymphoma [5]. Most discussed proteins

* *Corresponding author*. Tel.: +91 80 2293 2674; fax: +91 80 2360 0814.
** *Corresponding author*. Tel.: +91 821 2412191; fax: +91 821 2412191.
E-mail addresses: rangappaks@chemistry.uni-mysore.ac.in (K.S. Rangappa), sathees@biochem.iisc.ernet.in (S.C. Raghavan).
0006-2952/$ – see front matter
doi:10.1016/j.bcp.2008.10.018

responsible for leukemia and lymphoma in the recent past are Recombination Activating Genes (RAGs, the enzyme responsible for antibody diversity) [1,6–8] and Activation Induced Deaminase (AID, an enzyme responsible for somatic hypermutation and class switch recombination) [2,9–12].

Leukemia is one of the major types of cancer affecting a significant segment of the population, especially children. In fact, leukemia is the most frequent childhood cancer, with 26% of all cases, and 30% mortality [13]. Chronic myelogenous leukemia (CML), one of the most common leukemias, accounts for about 20% of all leukemia. CML is characterized by the presence of the Philadelphia chromosome, which is due to a reciprocal translocation between chromosome 9 and 22 [14]. Although the incidence rate for this disease remains relatively unchanged, some success has been attained in its treatment. The past two decades have seen a dramatic change in cancer treatment paradigms. For example, Imatinib (Gleevac), a drug developed specifically against the activated tyrosine kinase in CML is one of such major advances [15]. In addition, many other compounds have also been identified and clinically tested.

Although, the success of clinical trials in identifying new agents and treatment modalities has been significant, current treatments have many limitations. This includes side effects induced by the drugs and the development of acquired drug resistance [16]. Thus, the need for the development of effective anticancer therapeutic agents with well-defined pharmacokinetic properties is of importance.

Currently, there are many ways by which a drug is tested for its effectiveness as a cancer therapeutic agent. To this end, different apoptotic pathways leading to the cytotoxicity have been studied extensively for many compounds [17]. Recently, many chemotherapeutic compounds have been shown to have antiproliferative effects by inhibiting cell cycle at certain checkpoints [18]. Similarly, certain compounds are believed to function via cell cycle-mediated apoptosis [19,20].

Hydantoin derivatives possess a wide array of important biochemical effects and interesting pharmacological properties. For instance, several derivatives (phenytoin, mephenythoin, norantoin, methetoin, fosphenytoin) are well-known anticonvulsive drugs [21] and other hydantoin derivatives are found as antiarrhythmics, antimicrobial agents, skeletal muscle relaxants and nonsteroidal antiandrogens [22]. They also exhibit antidepressant, antiviral, antithrombotic activities as well as inhibitory activity against some enzymes (human aldose reductase and human leucocyte elastase) [23]. Some of the bicyclic [5,5] hydantoin scaffold having fluorine and chlorine are found to be potent inhibitors of the LFA-1/CAM interaction and farnesyl transferase [24].

Although hydantoin compounds are studied extensively, there are not many studies to investigate their anticancer properties. Recently, the cytotoxic activity of the spirohydantoin derivatives were tested in ovarian and breast cancer cells [25]. In addition to this, Carmi et al. investigated the effects of some of the 5-benzylidene-hydantoin derivatives on inhibition of the EGFR kinase activity and antiproliferative effects towards A431 cells [26]. It was found that, the exocyclic double bond is essential for both enzyme and cell growth inhibition, suggesting that, a rigid planar system is necessary to interact with the molecular target. To acquire more information about the cytotoxic potential of hydantoin derivatives, design and synthesis of novel analogs with various substituents at different positions are of prime importance.

The unique character of fluorinated molecules in medicinal chemistry is well recognized [27–32]. The presence of fluorine in biologically active molecule is shown to play a critical role in its pharmacological properties [33]. Our recent studies on the synthesis of different substituted diazaspiro hydantoin derivatives and evaluation of their antitumor activities unraveled that the fluorine substituted hydantoin analogs possessed potent antitumor activity [34]. Inspired by these results, we have designed a set of new series of more constrained diazaspiro bicyclo hydantoin derivatives containing different side chains at N-3 (acetic acid propyl ester, methoxy ethane, pentene) and N-8 (phenyl ring with electronegative atoms) positions. To determine how the steric and electronic properties of the side chain may influence its effect on the cell viability, we have analyzed cytotoxic and structure activity relationships (SARs) of all these derivatives against human leukemia cells [35]. Based on these studies, we have identified two compounds, 8-(3,4-difluorobenzyl)-1′-(pent-4-enyl)-8-azaspiro[bicyclo[3.2.1] octane-3,4′-imidazolidine]-2′,5′-dione (DFH) and 8-(3,4-dichlorobenzyl)-1′-(pent-4-enyl)-8-azaspiro[bicyclo[3.2.1]octane-3,4′-imidazolidine]-2′,5′-dione (DCH) (Fig. 1) with considerable antitumor activity. Therefore, in the present study, the mechanistic aspects of anticancer property of DFH and DCH are investigated in different human leukemia cells including CML. Here, we report for the first time that the fluorinated spirohydantoin derivative induces cytotoxicity in chronic myelogenous leukemia by inhibiting the cell growth probably by interfering with DNA replication. Further, the likely mechanism leading to the induction of apoptosis is discussed.

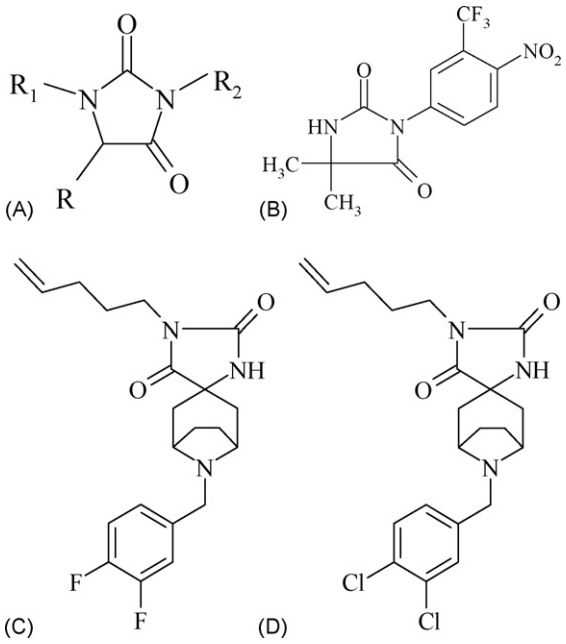

Fig. 1 – Chemical structures of DFH and DCH. (A) Structure of hydantoin, (B) chemical structure of Nilutamide, (C) chemical structure of DFH and (D) chemical structure of DCH. DFH and DCH are the derivatives of hydantoin in which basic moiety of Nilutamide was added.

2. Materials and methods

2.1. Chemicals and reagents

Unless otherwise mentioned, all the chemicals used in the present study were from Sigma–Aldrich, USA. Tritiated thymidine ([^{3}H] thymidine) was purchased from BRIT, India. Annexin V-FITC and antibodies were purchased from Santa Cruz Biotechnology, USA.

2.2. Synthesis and characterization of spirohydantoin derivatives (DFH and DCH)

The synthesis of diazaspiro bicyclo hydantoin derivatives was described earlier [35]. The formation of the hydantoin ring was confirmed by spectral analysis [35] (Fig. 1).

2.3. Cell lines and culture conditions

The Philadelphia chromosome positive, chronic myeloid leukemia cell line, K562 was used for every study. In addition to this, Reh (B-cell leukemia), CEM (T-cell leukemia) and 8E5 (Lymphocytic leukemia) cell lines were also used for some experiments and are mentioned in the respective ''figure legend''. K562, CEM and 8E5 cell lines were purchased from National Center for Cell Science, Pune, India. Reh cell line was a kind gift from Prof. Michael Lieber, University of Southern California, USA. All the cell lines were cultured in RPMI1640 (SERA LAB, UK) containing 10% FBS (GIBCO BRL, USA), 100 U of Penicillin G/ml and 100 μg of streptomycin/ml (Sigma–Aldrich, USA) at 37 °C in a humidified atmosphere containing 5% CO_2.

2.4. Trypan blue exclusion assay

The effect of DFH and DCH on proliferation of different leukemic cells was determined by Trypan blue exclusion assay. K562, Reh, CEM and 8E5 cells were seeded at a density of 1×10^5 cells/ml, cultured for 24 h and compounds were added at a concentration of 10, 50,100 and 250 μM. DMSO (Sigma–Aldrich, USA) was used as the vehicle control. Cells were collected at intervals of 24 h and resuspended in 0.4% Trypan blue (Sigma–Aldrich, USA). The number of viable cells was counted by using haemocytometer. IC_{50} values (concentration of compound causing 50% inhibition of cell growth) were estimated after 48 and 72 h of treatment with the compounds (Table 1). Each experiment was repeated a minimum of 3 times and the values obtained were plotted as a function of time.

Table 1 – IC_{50} value of DFH and DCH as determined based on multiple assays. IC_{50} was calculated based on Trypan blue and MTT assays at 48 and 72 h. Cell lines used are indicated in the first column.

Cell line	IC_{50} value (μM)			
	DFH		DCH	
	48 h	72 h	48 h	72 h
K562	80	28	120	35
Reh	110	44	148	54
CEM	100	35	125	40
8E5	90	45	140	60

2.5. MTT assay

Cytotoxic effect of DFH and DCH on K562, Reh, CEM, and 8E5 cells was further assessed using 3-(4,5-dimethylthiazol-2-yl)-2,5-diphenyl tetrazolium bromide (MTT) assay [36]. Cells were seeded in duplicates in 96-well plates at 1×10^4 cells/well. After 24 h, DFH and DCH were added at a concentration of 10, 50, 100 or 250 μM and incubated for 72 h. MTT reagent (5 mg/ml, Sigma–Aldrich, USA) was added and incubated for additional 4 h. The blue MTT formazan precipitate was then solubilized in detergent containing 50% N,N-dimethylformamide (Sigma–Aldrich, USA) and 10% of sodium dodecyl sulphate (Amresco, USA) and incubated for 2 h. Absorbance was measured at 570 nm on a multiwell ELISA plate reader (Molecular Devices, USA) scanning spectrophotometer. Cells grown in culture media alone or with appropriate concentrations of DMSO were used as controls. The percentage cell proliferation was calculated as a ratio of OD value of sample to the OD value of control.

2.6. LDH release assay

Release of lactate dehydrogenase (LDH) is an indicator of membrane integrity and hence cell injury. LDH assay was performed to assess the LDH release to the media following DFH treatment (10, 50,100 and 250 μM) on K562 cells for 24, 48 and 72 h and it was measured using standard protocols [37]. The intracellular LDH was determined after lysing the cells by freezing at −80 °C and rapid thawing. The LDH release was measured at an absorbance of 490 nm. The percentage of LDH release was calculated as: (LDH activity in media)/(LDH activity in media + intracellular LDH activity) × 100%.

2.7. [^{3}H] Thymidine incorporation assay

DNA synthesis was monitored by labelling cells using [^{3}H] thymidine. Cells were seeded in duplicates in a volume of 0.125 ml (1×10^5 cells/ml). DFH or DCH were added (10, 50, 100, 250 μM) after 24 h. The [^{3}H] thymidine (1 μCi) was added after 8 h of treatment. Following 48 h of incubation, the cells were pelleted, washed and resuspended in 5% TCA (Amresco, USA). The cells were resuspended in 50 μl of ice cold PBS after centrifugation, loaded on to filter paper discs (Sartorius, Germany), used for scintillation counting. The radioactivity count was expressed as disintegrations/min.

2.8. Cell cycle analysis

Cellular DNA content was measured by flow cytometry. Cells were cultured as described above and were treated with 10, 50, 100, 250 μM concentrations of DFH and DCH. Cells were harvested after 24, 48 and 72 h of treatment, washed, fixed in 70% ethanol and incubated with RNase A (Sigma–Aldrich, USA). Propidium iodide (PI, 50 μg/ml, Sigma–Aldrich, USA) was added half an hour before acquiring the flow cytometric reading (FACScan, BD Biosciences, USA). A minimum of 10,000

cells were acquired per sample and histograms were analyzed by using WinMDI 2.8 software.

2.9. Annexin V-FITC flow cytometric analysis

Annexin V-FITC apoptosis detection kit (Santacruz, USA) was used to detect early and late apoptosis. The annexin V has a strong affinity for phosphatidyl serine which is externalized in the membranes of apoptotic cells. In brief, after 24, 48 and 72 h of treatment with DFH (50 and 250 μM), cells were washed in PBS and resuspended in binding buffer (HEPES–NaOH 10 mM pH 7.4, 144 mM NaCl and 25 mM $CaCl_2$). Annexin V-FITC (0.2 μg/μl) and PI (0.05 μg/μl) were added and incubated in dark for 20 min. Cells were then subjected to FACS analysis. At least 10,000 events were recorded and represented as dot plots.

2.10. Confocal microscopy

Confocal microscopy was performed to visualize the early and late apoptotic cells. DFH treated cells were resuspended in binding buffer and stained with annexin V-FITC and PI as described above. The cells were then mounted over glass slide and observed under confocal laser scanning microscope (Ziess LSM 51^{MK4}, Germany).

2.11. DNA damage analysis by comet assay

Comet assay was performed based on the studies described earlier [38]. After 72 h of treatment with DFH, cells were collected, washed and mixed with low melting agarose (0.5%, Sigma–Aldrich, USA) and spread on agarose (1.5%, Sigma–Aldrich, USA) precoated slides. The slides were placed on ice for 10 min and submerged in lysis buffer (2.5 M NaCl (Amresco, USA), 100 mM EDTA (Sigma–Aldrich, USA), 10 mM Tris (Sigma–Aldrich, USA), 10% DMSO and 1% Triton X-100 (Sigma–Aldrich, USA), pH 10 at 4 °C) for more than 1 h. Slides were then equilibrated in alkaline buffer (30 mM NaOH (Amresco, USA), 1 mM EDTA, pH > 13 at 4 °C), electrophoresed at 0.86 V/cm at 4 °C, neutralized, washed and dried. Slides were stained with PI (2.5 μg/ml) and observed under fluorescence microscope (Olympus BX51 Upright fluorescence microscope, USA).

2.12. DNA fragmentation assay

Apoptotic degradation of DNA was analyzed by agarose gel electrophoresis. Briefly, K562 cells were cultured in the presence DFH or DCH at 50, 100 and 250 μM for 72 h. Cells were harvested and genomic DNA was extracted using standard protocol. DNA was resuspended in 250 μl of TE buffer. The DNA samples were run on 1% agarose gel and visualized by ethidium bromide staining and photographed.

To quantify the percentage of nuclei undergoing DNA fragmentation upon treatment with the DFH or DCH (50, 100 and 250 μM), PEG/Hoechst assay was performed according to the standard protocol [39]. The genomic DNA from the above cells was mixed with PEG (2.5%, Sigma–Aldrich, USA) and NaCl (1 M). Following centrifugation, the supernatant containing fragmented DNA was removed and an equal volume of Hoechst dye solution (0.2 μg/ml, Sigma–Aldrich, USA) was added. The fluorescence of the samples was determined at 360 nm excitation, 460 nm emission on a SPEX Fluoromax-3 spectrofluorometer (Jobin Yvon Horiba, USA) and the percentage of DNA fragmentation was calculated.

2.13. Western blot analysis

Exponentially growing K562 cells were treated with DFH (100 μM) for 24, 48 and 72 h. Cells were harvested, washed with PBS, resuspended in RIPA buffer (25 mM Tris, pH 7.6, 150 mM NaCl, 1% NP-40 (SRL, India), 1% Sodium deoxycholate (Sigma–Aldrich, USA) and 0.1% SDS) containing protease inhibitors and incubated on ice. The cell suspension was sonicated and the supernatant containing proteins were collected by centrifugation. The protein concentration was determined by Bradford method.

For Western blot analysis, ~40 μg protein was resolved over 8–10% SDS-polyacrylamide gel. Following gel electrophoresis, proteins were transferred to PVDF membrane (Millipore, USA), probed with appropriate primary antibodies (human reactive tubulin, PCNA, BAD, BCL2, procaspase 3, caspase 9, p-histone H3, Ku70, Ku80 from Santa Cruz Biotechnology; caspase 8, p53 and poly (ADP-ribosyl) polymerase (PARP) from Calbiochem, USA) as per standard protocols. The blot was developed using chemiluminescent solution (Immobilon™ western, Millipore, USA) and scanned by gel documentation system (LAS 3000, FUJI, JAPAN). Blots were stripped subsequently as per standard protocols and reprobed with anti-tubulin.

2.14. Statistical analysis

The results are expressed as the mean plus or minus standard error. All analyses were performed with the GraphPad software using one-way ANOVA followed by Tukey–Kramer Multiple Comparison Test. Statistical significance was considered at $p < 0.05$.

3. Results

3.1. DFH and DCH induces cytotoxicity on leukemic cells

Induction of cell death or inhibition of cell proliferation is an important property for chemotherapeutic agents. In the present study we have used both DFH and DCH (Fig. 1) to understand the mechanism of its cytotoxicity. K562, a leukemic cell line derived from a chronic myelogenous leukemia patient has been used extensively in the current study. However, other leukemia cell lines have also been used in certain experiments.

Trypan blue assay was the first line of our investigation, where we assessed the effect of DFH and DCH on cell viability of different leukemic cell lines (K562, Reh, CEM and 8E5). To investigate the potential effects of DFH and DCH, the cells were treated with 10, 50, 100 and 250 μM of each compounds. The cells without the addition of the compound were used as controls for each cell line. Since the compounds were dissolved in DMSO, the cells with DMSO (equivalent to DMSO used in 250 μM) were also used as vehicle control. The cells were counted at intervals of 24 h till they attained stationary phase. Results showed that addition of DFH and DCH affected

the viability of the cells remarkably in all four leukemic cell lines (Fig. 2A–H). The cell death induced by the DFH and DCH was in a dose- and time-dependent manner. In all the cell lines tested, the lowest concentration (10 μM) of DFH and DCH was least effective (Fig. 2). However, an increase in the concentration of DFH or DCH to 50 or 100 μM affected the cell viability dramatically within 48–72 h, whereas 250 μM showed complete inhibition at 48 h of treatment (Fig. 2). It was found that the effect was maintained even after prolonged incubation periods. Interestingly, the DMSO control, corresponding to the highest concentration of compound tested did not show any significant toxic effect (Fig. 2). These results suggest that both DFH and DCH induce cytotoxicity on the tested human leukemic cells, however, the effect was more prominent when DFH was used.

The cytotoxicity induced by DFH and DCH was further verified using MTT assay. In order to perform this we incubated K562, Reh, CEM and 8E5 cells with 10, 50, 100 and 250 μM of DFH

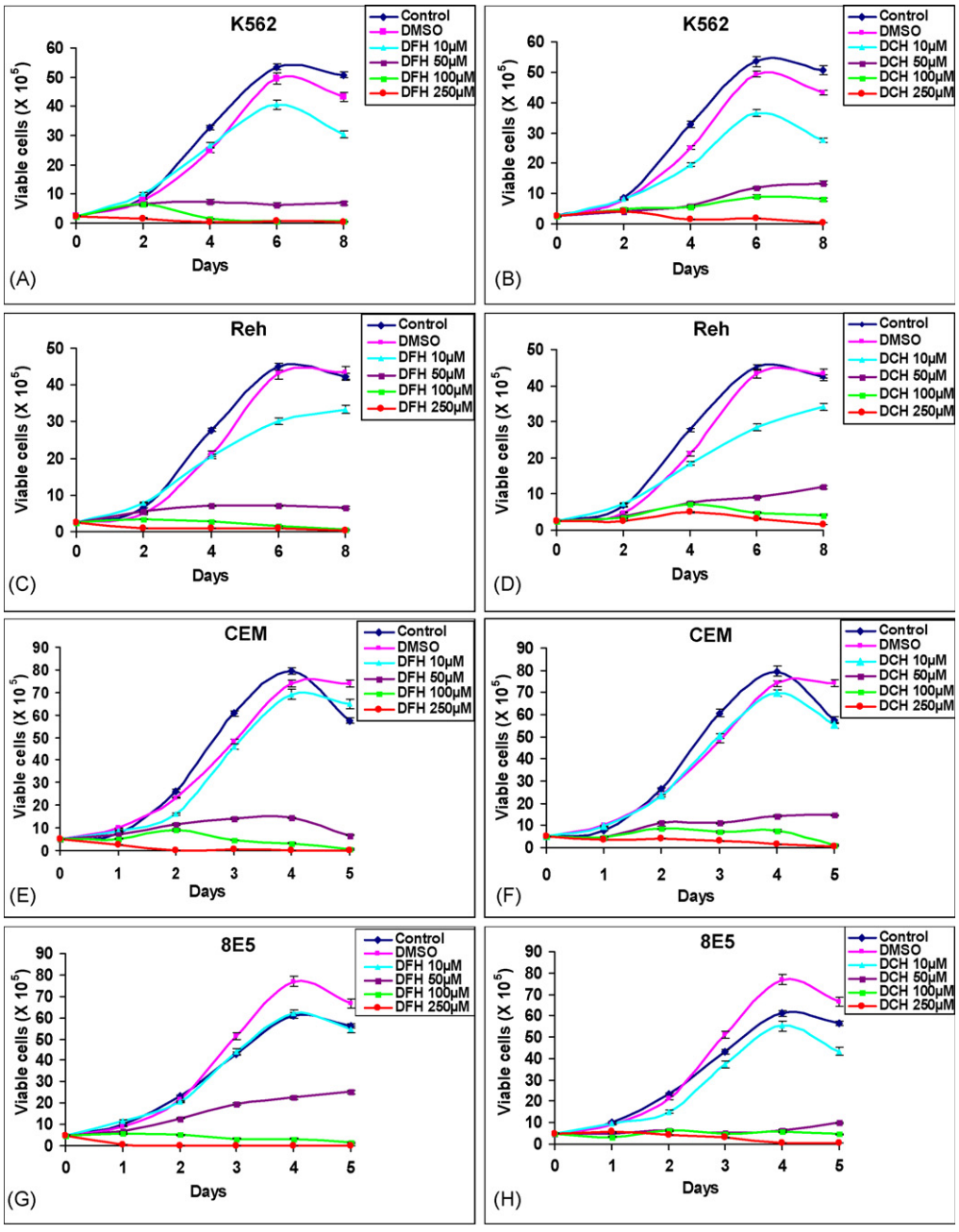

Fig. 2 – Dose and time-dependent effect of DFH and DCH on cell viability of different leukemic cells. Approximately 1×10^5 cells/ml were cultured at 37 °C. DFH and DCH were added after 24 h of plating at a concentration of 10, 50, 100 and 250 μM. In addition to the no compound control, DMSO treated cells were also used as vehicle control. From the time of addition of compounds, live cells were counted at an interval of 24 h, till the cells reached stationary phase and the data was represented as a graph. (A) K562 cells treated with DFH, (B) K562 cells treated with DCH, (C) Reh cells treated with DFH, (D) Reh cells treated with DCH, (E) CEM cells treated with DFH, (F) CEM cells treated with DCH, (G) 8E5 cells treated with DFH, and (H) 8E5 cells treated with DCH. Error bars are represented in the figure.

or DCH and cells were harvested at 72 h and used for the assay. Cell proliferation was estimated by the reduction of MTT by live cells. Results showed that after treatment with DFH or DCH, cell viability decreased dramatically from 50 μM onwards (Fig. 3). The observed inhibition was concentration dependent. These results further suggest that both DFH and DCH affect the viability of the cells. Based on the above studies the IC_{50} value for DFH in K562 cells were estimated to be around 80 and 28 μM when calculated at 48 and 72 h, respectively, while the same for DCH was 120 and 35 μM (Table 1). IC_{50} value for other cell lines are also calculated and presented in Table 1.

Further LDH release assay was performed to test the cell damage induced by DFH. For this, K562 cells were cultured with 10, 50, 100 and 250 μM of DFH for 24, 48 and 72 h and release of LDH (an indicator of membrane integrity) was measured. Results showed a dose- and time-dependent increase in LDH release, further confirming the above results (Suppl. Fig. 1).

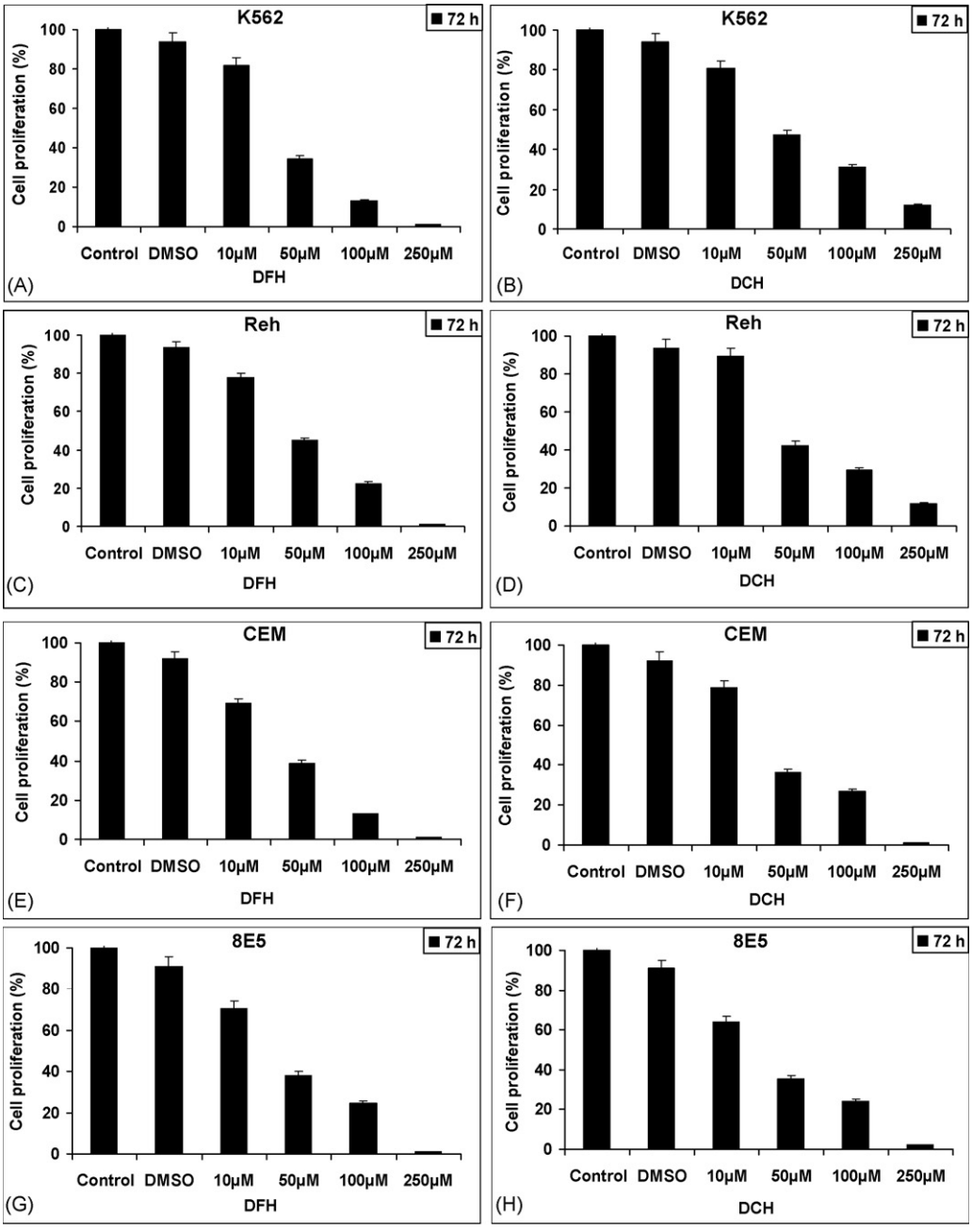

Fig. 3 – Determination of the effect of DFH and DCH on proliferation by MTT assay. After 72 h of exposure, cells with DFH and DCH (10, 50, 100 and 250 μM concentrations), were incubated with MTT (5 mg/ml) in duplicates and resulting blue formazan precipitate was dissolved in detergent and absorbance was measured at 570 nm. Results are presented as percentage of cell proliferation (the cell viability of vehicle cells were regarded as 100%). (A) K562 cells treated with DFH, (B) K562 cells treated with DCH, (C) Reh cells treated with DFH, (D) Reh cells treated with DCH, (E) CEM cells treated with DFH, (F) CEM cells treated with DCH, (G) 8E5 cells treated with DFH, and (H) 8E5 cells treated with DCH. Error bars are represented in the figure.

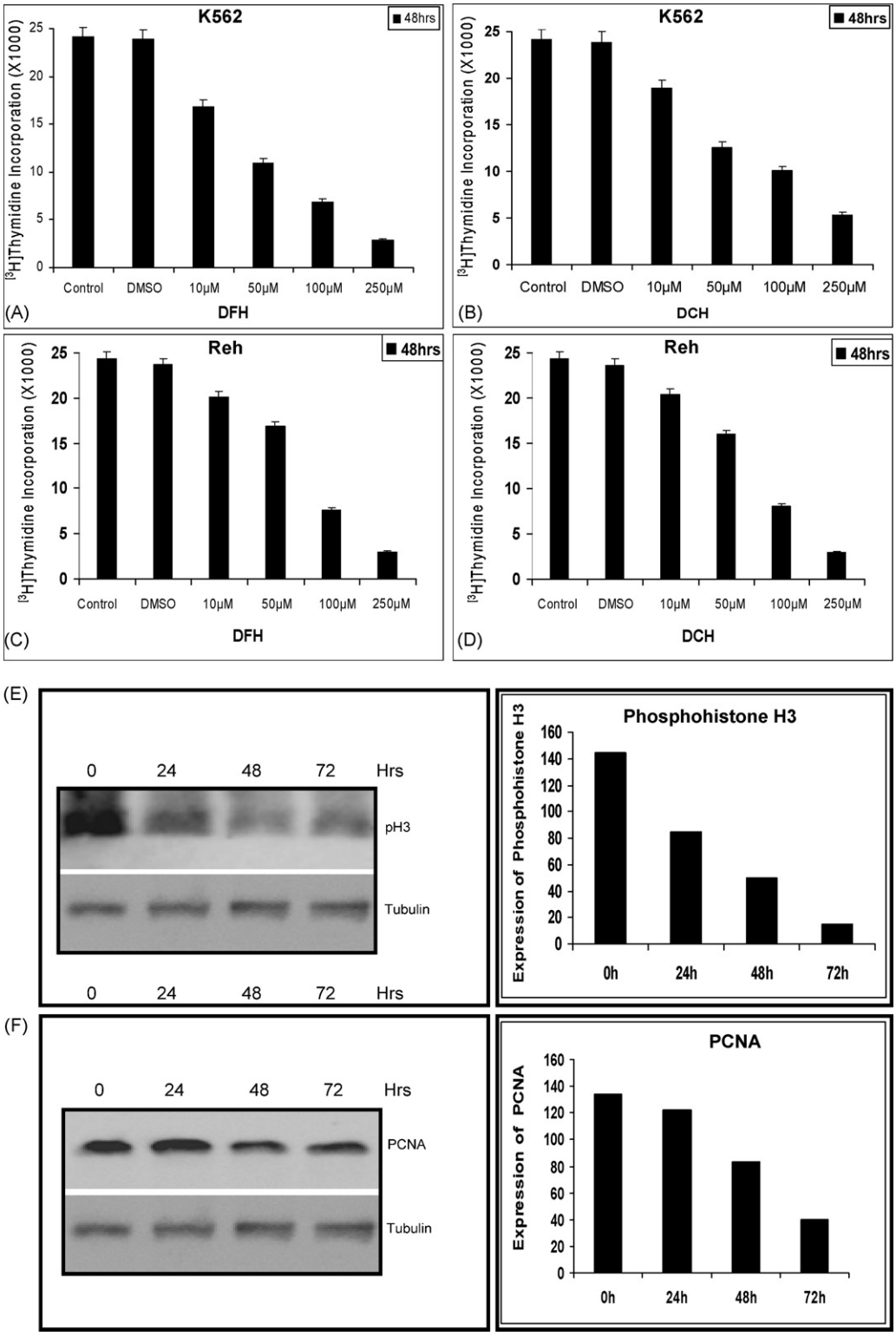

Fig. 4 – DFH and DCH treatment in leukemic cell lines affect proliferation of the cells. DFH and DCH (10, 50,100 or 250 μM) were added to K562 or Reh cells after 24 h of culture. After 8 h of addition of the compounds, tritiated thymidine was added. Cells were harvested after 48 h and processed. The incorporation of radioactivity was measured in a β scintillation counter and the results were expressed as mean counts/min. (A) and (B) are incorporation of [^{3}H] thymidine in K562 cells after addition of DFH and DCH, respectively. (C) and (D) are incorporation of [^{3}H] thymidine in Reh cells upon treatment with DFH and DCH, respectively. (E and F) Western blot analysis of proteins, related to DNA replication. Cell lysate was prepared from K562 cells after culturing with 100 μM of DFH for 24, 48 and 72 h. DMSO treated cells grown for 72 h was used as control. Equal amounts of cellular proteins (40 μg/lane) were resolved by SDS-PAGE and transferred to a PVDF membrane. The membrane was probed for the expression of p-histone H3 (E) and PCNA (F) with specific primary antibodies and secondary

3.2. DFH and DCH affect proliferation of leukemic cells

One of the methods used to study cell proliferation is based on incorporation of radio labelled nucleotides into the DNA of dividing cells. Since we have noticed that DFH and DCH affect the viability of the cells, we were interested to know whether it can affect the cell division or directly induce cell death by apoptotic pathways. To test this, we cultured K562 or Reh cells in the presence of [^{3}H] thymidine after the addition of DFH or DCH. Results showed that both the compounds at 50, 100 and 250 μM reduced the incorporation of [^{3}H] thymidine after 48 h of its addition, however, to a limited extent (Fig. 4A–D). These results indicate that one of the ways of induction of cytotoxicity by DFH and DCH could be by inhibiting cell division. However, in addition to this it also might be inducing apoptosis.

Since our data suggested that DFH and DCH might interfere with DNA replication, we were interested in checking the status of some of the replication related proteins in K562 cells. Since DFH was showing the most prominent effect on cell division in K562 cells, for Western blot analysis we have used only the DFH treated cells. Cell lysate was prepared from K562, after treating with DFH for different time points (24, 48 and 72 h). Since p-histone H3 is a marker for cell division, we used anti-p-histone H3 to check its expression. The results showed that levels of p-histone H3 reduced upon treatment with DFH from 24 h onwards; however, robust expression was seen in the control (Fig. 4E). These results indicated that histone H3 (a histone normally phosphorylated at M phase) is not phosphorylated when cells were treated with DFH. Moreover, we noted that the levels of expression of PCNA, another protein required for replication was reduced upon treatment with DFH after 24 h (Fig. 4F). Further studies are required to understand the exact mechanism of inhibition of DNA replication induced by DFH.

3.3. Assessment of cell cycle profile upon treatment with DFH and DCH on leukemic cells

Data from Trypan blue exclusion assay and MTT assay showed that DFH and DCH induced reduction in the number of live cells. Tritiated thymidine incorporation assay further suggested that there is a reduction in cell proliferation. Studies on expression levels of replication related proteins further confirmed such a possibility. Based on this, we were interested in studying cell cycle distribution by fluorescence-activated cell sorting analysis of PI-labelled cells. K562, Reh, CEM and 8E5 cells were harvested after 72 h of compound treatment (10, 50, 100 and 250 μM) and were PI stained and subjected to flow cytometry. The histogram of control or DMSO treated cells showed a standard cell cycle pattern, which include G1 and G2 peaks separated by S phase peak (Suppl. Fig. 2). SubG1 peak (mostly dead cells) was either absent or not prominent. Interestingly upon addition of DFH to K562 cells, a concentration dependent change was observed in the cell cycle pattern (Suppl. Fig. 2A). However, such a change was less prominent when the cells were treated with DCH (Suppl. Fig. 2B). Comparable changes in the cell cycle distribution of DFH and DCH treated cells were also noted in the case of Reh, CEM and 8E5 cells (Suppl. Fig. 2C–H). Although we were not able to visualize prominent arrest at any stage of the cell cycle during this analysis, we noted that there was a remarkable accumulation of subploid cells, the subG1 phase (G0/G1) (Fig. 5D), and decline of both G1 (Fig. 5A) and G2/M (Fig. 5C) phases when compared with untreated cells. Upon close evaluation, we noted that at least in some cell lines there is a block in the S phase (Fig. 5B). Further, when DFH treated K562 cells were harvested after 24 and 48 h, we could observe an accumulation of cells both at G1 and S phase (Suppl. Fig. 3) and its mechanism needs to be explored further. Therefore, our studies confirm that growth inhibition could be mediated by a DNA replication defect followed by apoptosis.

3.4. DFH treatment leads to translocation of phosphatidyl serine to the outer membrane

Since we could observe accumulation of cells at G0/G1 peak during cell cycle analysis induced by DFH and DCH, we were interested in quantifying the different types of apoptotic cells. Phosphatidyl serine residues, which are normally located in the internal phospholipid layer are actively translocated to the external layer in apoptotic cells and thus can be detected by annexin-V staining. Since, both DFH and DCH did not show significant variation in cytotoxic properties, further experiments were performed using only DFH except, when it is mentioned otherwise. In order to detect and quantify the apoptosis induced by DFH, we have used annexin V-FITC/PI double staining. K562 cells were harvested after 24, 48 and 72 h of treatment with DFH (50 and 250 μM) and used for double staining followed by FACS analysis. Dot plot results of DFH on K562 cells showed a time- and dose-dependent increase in late apoptotic cells (Fig. 6A–C). Although there was an increase in early apoptotic cells the effect was less prominent (Fig. 6A–C, panel d). DFH induced effect was remarkable at 72 h of treatment, which showed that at a concentration of 50 μM, about 7.58% of cells were in early apoptotic stage (stained only by annexin V-FITC), which is 2.8-fold higher than DMSO treated controls (Fig. 6C, a and b), while about 15% of the cells were in late apoptotic stage (stained by annexin V-FITC and PI), which was 2.4 times higher than that of DMSO control (Fig. 6C, a and b). At a concentration of 250 μM this was observed to be 12.9% (4.8 times higher than control) and 68.6% (11 times higher than control), respectively (Fig. 6C, a and c). Comparable results were obtained when Reh cells were used for the study after harvesting at 72 h (Suppl. Fig. 4). These results suggested that DFH induces apoptosis. The annexin V/PI double stained cells indicate that in such cells extensive cell membrane damage has occurred, which results in nuclear staining. These conclusions were further verified by observing the above stained cells under a confocal microscope. The results showed that most of the K562 or Reh control cells

antibody. The α-tubulin was used as an internal loading control. Proteins were detected using enhanced chemiluminescence's method. In all panels, "0" is DMSO control; "24", "48", "72" are cells harvested after 24, 48 and 72 h of DFH treatment, respectively. For each protein, respective intensity of bands were quantified and presented as histogram.

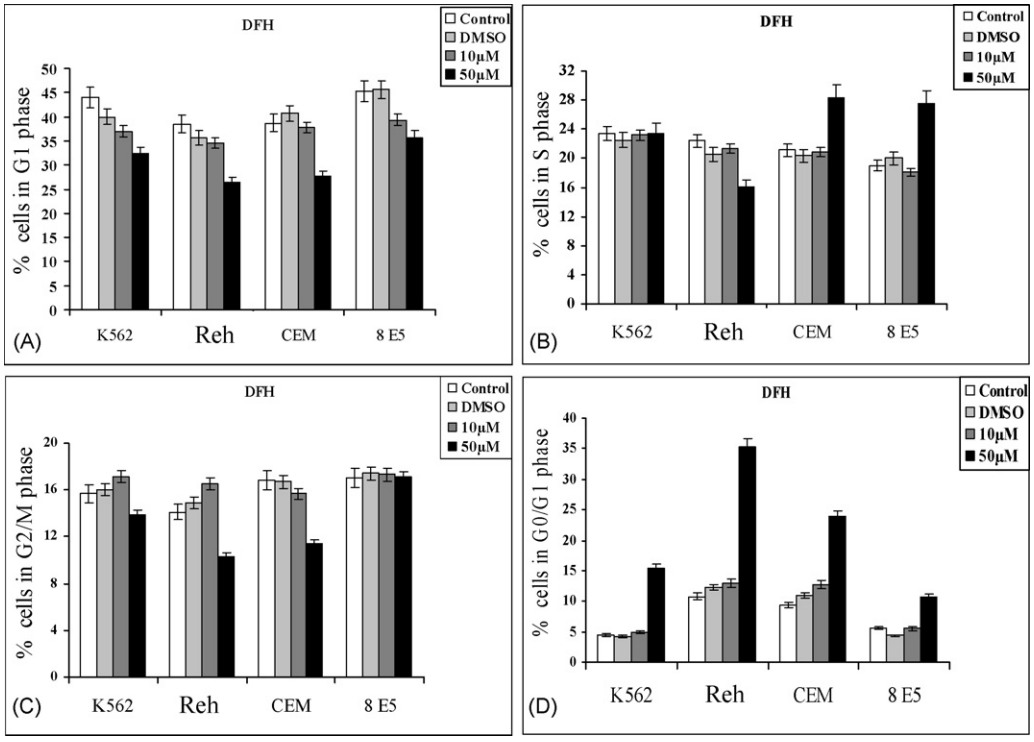

Fig. 5 – Cell cycle phase wise distribution of DFH and DCH treated leukemic cells. K562, Reh, CEM and 8E5 cells (1×10^5 cells/ml) were incubated at 37 °C with DFH (10 and 50 μM). Following 72 h of incubation, cells were fixed and stained with propidium iodide and sorted in a FACS machine. (A–D) Histogram comparing effect of DFH on specific cell cycle stages on different leukemic cell lines. G1 phase (A), S phase (B), G2/M phase (C) G0/G1 phase, (D) cell cycle distribution of K562, Reh, CEM and 8E5 cells. In the case of each cell line, control, DMSO treated control, 10 and 50 μM DFH treated samples are compared and plotted. Error bar is indicated.

(including DMSO treated) were negative for annexin V-FITC and PI (Fig. 6D, a and data not shown). At 50 μM concentration of DFH we could see cells stained by annexin V-FITC (green colored rim) and intact nuclei, suggesting damage of cell membrane (Fig. 6D, b). Results obtained from the cells treated with 250 μM of DFH, showed cells which were stained by both annexin V-FITC (green color) and PI (red color) suggesting complete damage of cell membrane (Fig. 6D, c and d). These results suggest a total disruption of cell membrane and further damage to the chromosomal DNA upon treatment with DFH.

3.5. *DNA fragmentation and strand breakage are induced by DFH*

The parameters which were considered to assess the DNA damage upon treatment with compounds were nuclear condensation and chromosomal DNA fragmentation. K562 cells treated with 100 μM of DFH were harvested after 72 h and used for single cell gel electrophoresis. Around 5–6 slides were observed from both normal and treated samples. Results showed the formation of comets when K562 cells were treated with DFH (Fig. 7B–D). We could also see nuclear condensation in cells where there was no comet (data not shown) which is also a marker for nuclear damage. Both nuclear condensation and comets were absent in control cells which were treated with DMSO alone (Fig. 7A). Comparable results were obtained when Reh and CEM cells were used in a similar study (data not shown).

DNA damage observed by comet assay was further verified by DNA fragmentation assay. The chromosomal DNA was extracted from the K562 cells treated with increasing concentrations (50, 100, 250 μM) of DFH after 72 h and used for agarose gel electrophoresis as described in Section 2. The results showed fragmentation of the DNA leading to a smear in the lanes in which cells were treated with DFH (Fig. 7E). The observed smear is the result of DNA breakage at multiple positions across the chromosomal DNA. The intensity of smear increased with the dose, 100 μM showing moderate smearing and 250 μM showing maximum (Fig. 7E), which was further quantified (Fig. 7G). DCH also showed smearing when treated with K562 cells, however, it was limited to a lesser extent (Fig. 7F and G). These results in conjunction with annexin V-FITC/PI staining further suggest that DFH induces fragmentation of chromosomal DNA leading to apoptosis.

3.6. *DFH induces regulation of the expression of apoptotic related proteins*

Since we have seen evidence for induction of apoptosis by DFH in the above experiments, we tested apoptosis specific proteins by immunoblot analysis. Cell lysate was prepared from K562 cells after treating with DFH for 24, 48 and 72 h as described in Section 2. Proteins were resolved on a denaturing PAGE, transferred to PVDF membrane and probed with antibodies of interest.

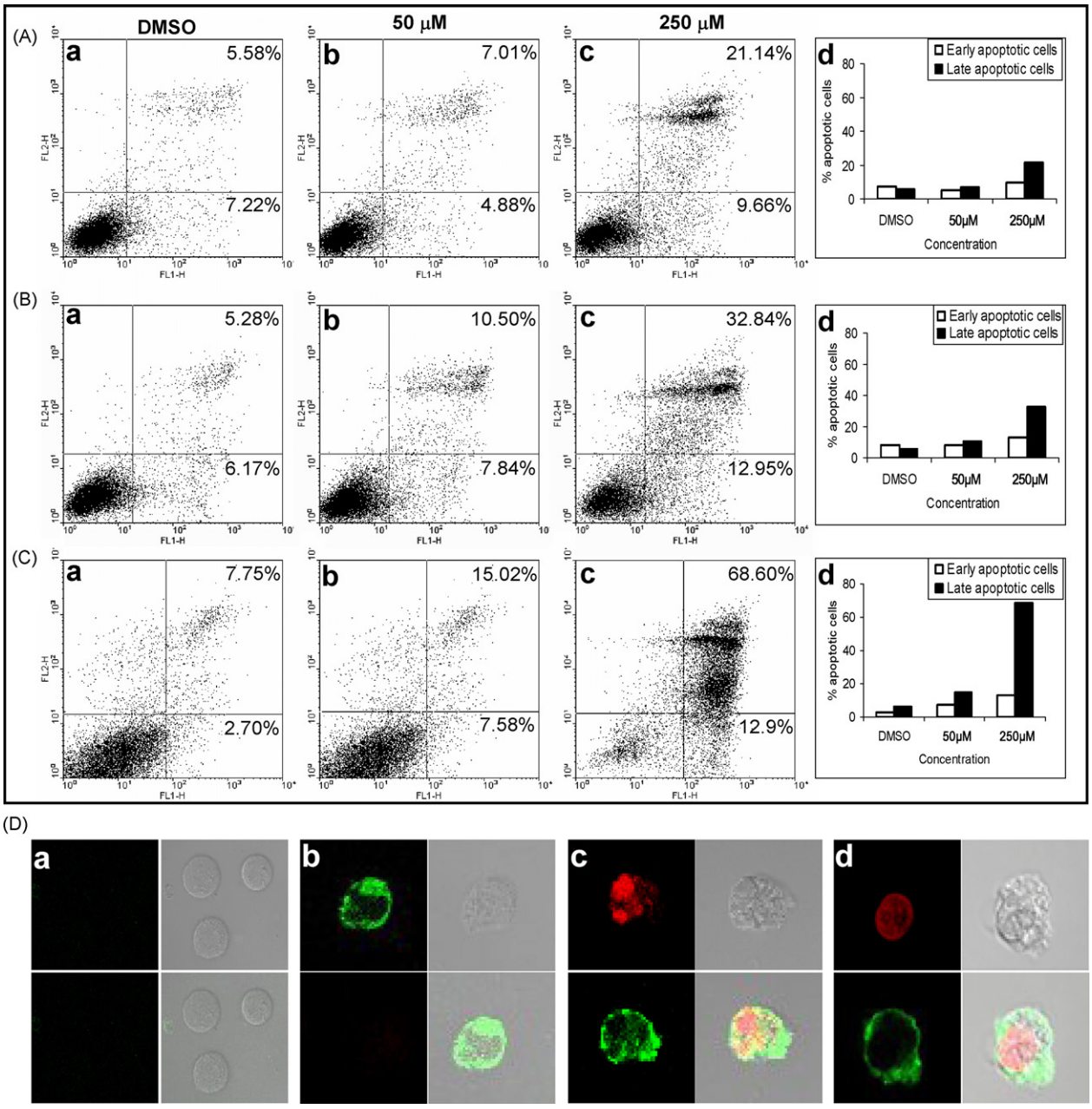

Fig. 6 – Detection of apoptosis induced by DFH in leukemic cells by flow cytometry and confocal microscopy. K562 cells were cultured with DFH (50 and 250 μM each) for 24 h (A), 48 h (B) and 72 h (C) and processed for annexin V-FITC/PI double staining. The cells were then quantitatively or qualitatively monitored. In each panel, lower left quadrant shows cells which are negative for both annexin V-FITC and PI, lower right shows annexin V positive cells which are in the early stage of apoptosis, upper left shows only PI positive cells which are dead, and upper right shows both annexin V and PI positive, which are in the stage of late apoptosis or necrosis. Panels shown are annexin V-FITC incubated with the K562 cells, which are treated with DMSO (a), annexin V-FITC and PI stained cells after incubation with 50 μM (b) or 250 μM of DFH (c) for different times. In all panels (d) is histogram showing comparison of early apoptotic and late apoptotic cells at different doses of DFH. (D) Visualization of apoptotic cells by confocal microscopy. As described above the K562 cells treated with DFH for 72 h were annexin V-FITC/PI double stained. Microscopic evaluation of the cells showed that most of the control cells were negative for both annexin V and PI indicating live cells with cellular integrity. DMSO treated cells stained with annexin V and PI (a), cells in the early apoptotic stage stained only with annexin V appeared green in color (b), cells in the late stage of apoptosis, stained with both annexin V and PI appeared red and green in color (c, d). (For interpretation of the references to color in this figure legend, the reader is referred to the web version of the article.)

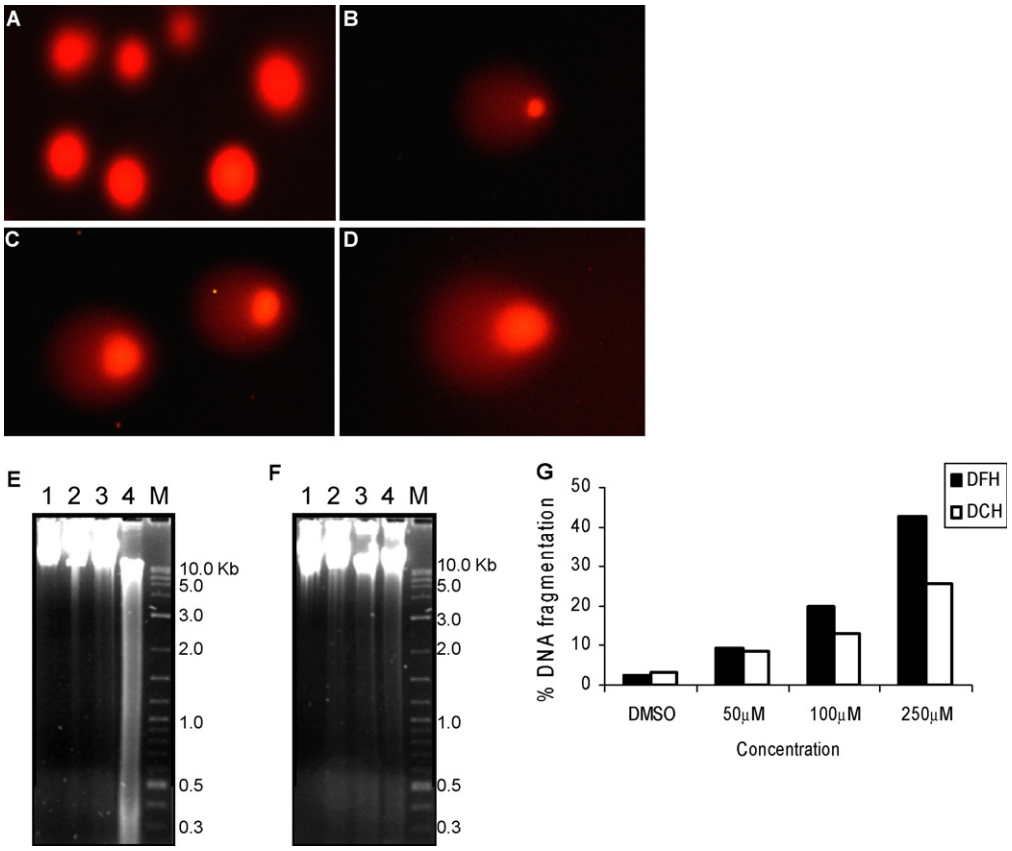

Fig. 7 – Detection of DNA damage in K562 cells induced by DFH. Comet assay. DFH treated K562 cells (72 h) were layered over a mini-agarose gel, lysed, electrophoresed in alkaline buffer and stained with propidium iodide. (A) Control K562 cells incubated with DMSO. (B–D) K562 cells treated with 100 μM of DFH. The DNA fragmentation resulting in a comet like appearance is seen in some cells. However, the number of such cells were limited as the DFH treatment killed most of the cells. (E, F) Agarose gel profile showing DNA fragmentation. The chromosomal DNA was extracted from K562 cells, which were treated with different concentrations of DFH (E) or DCH (F). The purified DNA was then resolved on a 1% agarose gel at 30 V for 6 h. In both panels, K562 cells were treated as follows. Lane 1: DMSO; Lanes 2–4: 50, 100 and 250 μM, respectively. "M" is Marker. (G) Quantification of the fragmented DNA. The extent of DNA fragmentation due to DFH and DCH treatment (50, 100 and 250 μM) on K562 cells was quantified by Hoechst staining followed by fluorimetry and represented in a histogram.

Immunoblot analysis of DFH treated samples prepared after 24, 48 and 72 h showed downregulation of the anti-apoptotic protein, BCL2, when compared to control (Fig. 8A). When the blot was reprobed with BAD, a proapoptotic protein, we found a time-dependent upregulation in its expression (Fig. 8A). These results further confirm the activation of apoptosis upon treatment with DFH.

Caspase 8 is a protein known to be activated if apoptosis is mediated by extrinsic pathway. Hence, we were interested to test whether DFH induces caspase 8 activation. Upon immunoblot analysis, we could not find any cleaved product other than the precursor form (Fig. 8B). Thus, it appears that DFH induced apoptosis would not be through the extrinsic pathway. Poly (ADP-ribosyl) polymerase is a single-strand break repair enzyme (116 kDa). It is known that upon activation of apoptotic pathway, caspase cleaves PARP into 85 and 27 kDa polypeptides [40]. By immunoblotting using anti-PARP, we found that the addition of DFH led to prominent PARP cleavage, resulting in accumulation of the 85 kDa product (Fig. 8C). The PARP cleavage was observed from 48 h post treatment. However, 24 h of treatment did not induce any PARP cleavage as seen in DMSO treated control (Fig. 8C). Since PARP cleavage requires activation of caspase, we were interested in testing the level of procaspase 3 in DFH treated cells. Results showed a noticeable time-dependent activation of procaspase 3, starting from 24 h onwards (Fig. 8D). Since the antibody used against procaspase 3, could not recognize its cleaved products we were unable to detect cleaved caspase 3 products. When the same blot was probed with caspase 9 we could see both activated and cleaved form of caspase 9 in a time-dependent manner (Fig. 8D). Reprobing with anti-tubulin antibody, the loading control, confirmed that the amount of protein loaded was equal in all the experiments (Fig. 8). Therefore, immunoblot analysis suggests that DFH induces activation of proapoptotic proteins and downregulation of antiapoptotic proteins to induce apoptosis in chronic myelo-

genous leukemia cells, K562. Activation of apoptosis by DFH was mediated through caspase 3 and 9 activation following PARP cleavage.

We also found that DFH induced accumulation of p53 in a time-dependent manner. We could observe the induction as early as 24 h post treatment of DFH (Fig. 8E). There are few studies in the literature speculating that K562 cells are null for p53. However, it is important to point out that some of the subclones derived from K562 cells are positive for p53. Therefore, it is not surprising to see the observed expression of p53 in K562 cells in our experiments. Ku70 and Ku80 are DNA end binding proteins involved in nonhomologous end joining, a pathway involved in DNA double-strand break repair in mammalian cells. Earlier studies have shown that upon activation of apoptosis, these proteins get down regulated. Hence, we were interested in testing the expression levels of both Ku70 and Ku80 upon treatment with DFH. Following Western blot analysis we could observe the reduced level expression of both Ku70 and Ku80 (Fig. 8F). These results, further suggest that DFH treatment leads to the down-regulation of Ku proteins and hence promotes apoptosis in K562 cells.

4. Discussion

Hydantoin derivatives are used widely in treating many human diseases. However, there are only few studies to look into their anticancer properties. In the present study, we have shown that novel hydantoin derivatives, DFH and DCH possess cytotoxic effects on many leukemic cell lines including CML. We found that both the compounds affect DNA replication leading to inhibition of cell growth. Translocation of phosphatidyl serine, fragmented nuclear DNA and altered levels of various apoptotic proteins and repair proteins further suggest that these compounds could induce apoptosis.

To explore the antiproliferative property of DFH and DCH, first we checked for cell viability by Trypan blue exclusion assay, cell damage by LDH release assay and cell proliferation by MTT assay. Our results showed that cell death induced by DFH and DCH was time- and concentration-dependent. In addition to DFH and DCH, a comparable phenomenon has also been observed for other compounds tested as potential anticancer drugs [41].

4.1. *Does DFH inhibit cell growth in leukemic cells by affecting DNA replication?*

Reduced incorporation of tritiated thymidine shows that both DFH and DCH are able to inhibit the proliferation of cells. Although this does suggest that DFH could induce a block during cell division, results based on cell cycle analysis using flow cytometry did not show any prominent arrest in the cell cycle. Nevertheless analysis of individual peaks of cell cycle indicated a transient arrest at S phase at 72 h of DFH treatment (Fig. 5B). Besides it appears that there could be S and G1 arrest at early time points, which need to be addressed further at the molecular level. The probability of a replication arrest was considered further. A reduction in the expression of PCNA, a protein involved in DNA replication supports this notion [42]. However, the observed maximum reduction in PCNA level was only about 40%. Perhaps this perfectly explains, why we could not observe any prominent cell cycle arrest. The reduction in the level of p-histone H3 after the treatment with DFH further supports the possible effect during DNA replication. Similar to PCNA, in this case also reduction in the expression of p-histone H3 was limited. Histone H3 is normally phosphorylated at M phase and is used as a marker for mitotic phase [43]. Since DFH treatment prevents cell cycle progression beyond S phase in many cells, the observed reduced expression of p-histone H3 is of interest. However, further studies are required to understand the exact mechanism of its action.

4.2. *Does DFH mediate cytotoxicity due to altered expression of apoptotic proteins?*

One of the most interesting observations of cell cycle analysis was the dramatic increase in subG1 (G0/G1) peak in a concentration dependent manner, which suggested the presence of apoptotic cells. Annexin V-FITC staining is capable of detecting apoptosis, thus revealing the type of cell death induced by the compound of interest. The combination of annexin V-FITC and PI has been used to discriminate early apoptotic cells from late apoptotic and necrotic ones, based on the translocation of phosphatidyl serine from the inner to the outer layer of the plasma membrane of early apoptotic cells which is stained by annexin V [44]. We compared the apoptosis inducing potential of DFH by annexin V-FITC and PI double staining using both flow cytometry and confocal microscopy. We could observe early and late apoptotic cells suggesting that DFH can induce apoptosis in CML cells. In addition to that the cells exhibited the ultra structure and biochemical features which are characteristic to apoptosis, as shown by loss of cell viability, chromatin condensation and inter nucleosomal DNA fragmentation.

BCL2 family is the best characterized group of apoptosis related proteins [45]. According to the functional properties there are two main groups; antiapoptotic proteins such as BCL2 and BCL-X_L and proapoptotic proteins such as BAD, BAX, and BID. BCL2 proteins interact with other molecules through their BH-3 domain, which is important for the regulation of apoptosis [46]. Generally BCL2 is expressed in higher levels in cancer cells [47]. In our studies we see that DFH down regulates BCL2 in a time-dependent manner promoting apoptosis. As expected, we see an upregulation of BAD, a proapoptotic protein, upon treatment with DFH. Upregulation of proapoptotic proteins and downregulation of antiapoptotic proteins induced by different anticancer agents have been reported earlier in many cancers including pancreatic carcinoma [48]. Therefore, the observed alterations in the levels of both proapoptotic and antiapoptotic proteins by hydantoin derivatives is an important finding further supporting its use as an apoptosis inducing anticancer agent.

Caspase 3 activation and cleavage of PARP are considered as other markers for apoptosis [49]. In mammals generally apoptosis is a result of proteolysis of various cellular components by activated caspases, which are a set of cysteine proteases [50]. Caspase 3, 8 and 9 are some of caspases, which we have studied in our investigation. Our results showed the apoptosis induced by DFH on CML cells was associated with

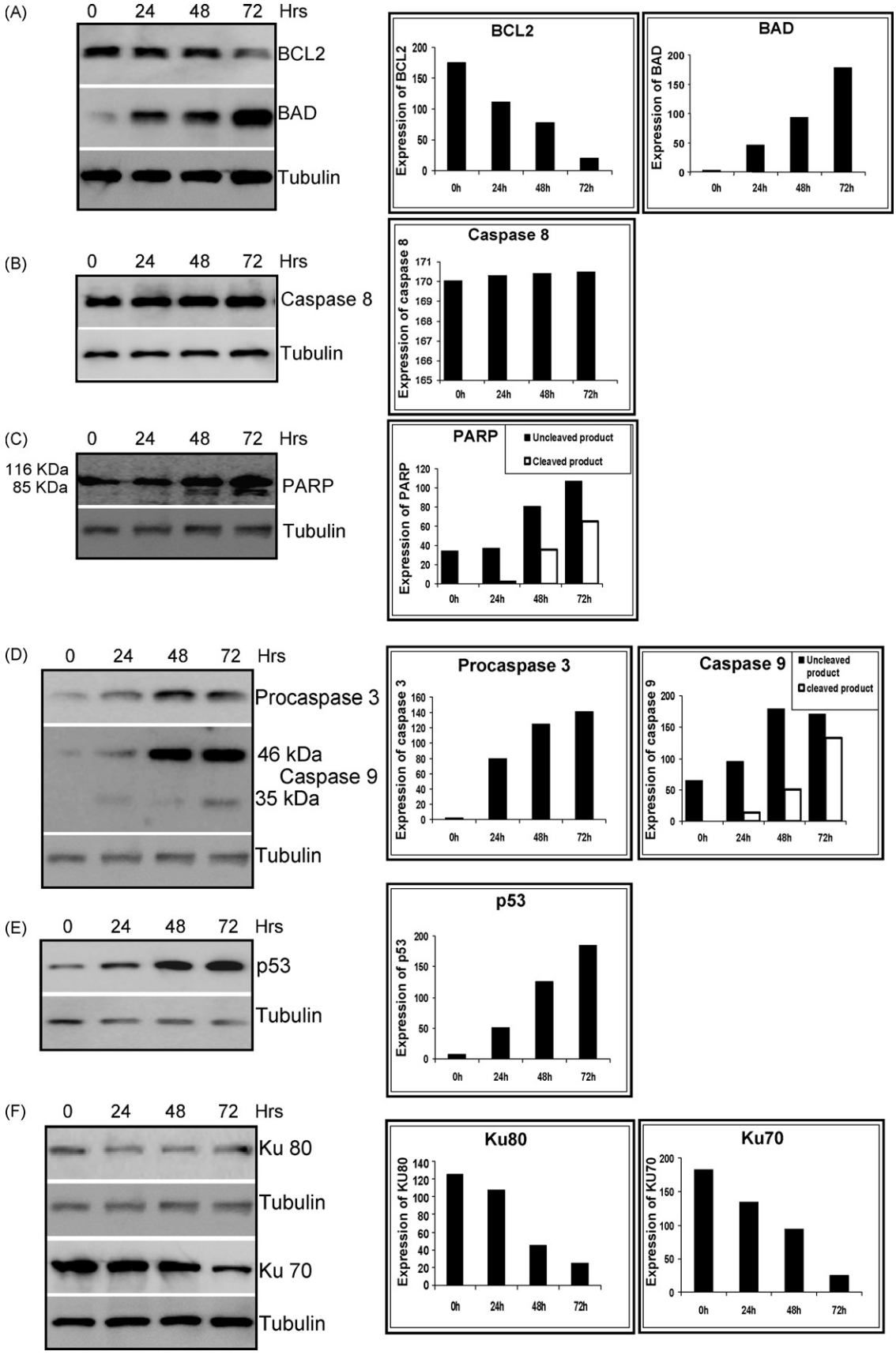

Fig. 8 – Effect of DFH on the expression of apoptotic proteins in K562 cells. Cell lysate was prepared from K562 cells after culturing with 100 μM of DFH for 24, 48 or 72 h. DMSO treated cells grown for 72 h was used as control. Equal amounts of cellular proteins (40 μg/lane) were resolved by SDS-PAGE and transferred to a PVDF membrane. The membrane was probed

marked activation of cleavage of caspase 9 and activation of procaspase 3. Since the antibody used was not against the cleaved region of caspase 3 we could not detect the cleaved product. However, we were able to detect the activated caspase 9 and its cleaved products.

PARP is shown to have a role in DNA damage induced apoptosis and is one of the major targets of caspase 3 [51]. We find that DFH treatment induced PARP cleavage, which further suggests the activation of caspase 3. Activation of caspase 3 requires an active caspase 9, which was also demonstrated by our experiments. Therefore, it appears that treatment with DFH triggers activation of mitochondrial pathway of apoptosis. In addition, the observed lack of caspase 8 cleavage, rules out the activation of the extrinsic pathway (Fig. 9).

We could also observe a time-dependent upregulation of p53 upon treatment with DFH in K562 cells. Mutations in p53 are a common genetic change found in most of the human cancers [52]. Therefore, why would DFH elevate the expression of p53 for inducing apoptosis? In recent past there are few reports suggesting that expression of wild type p53 is needed for induction of cytotoxicity of many cancer therapeutic agents [53]. In a recent study using gefitinib it was reported that p53 induction was able to enhance the expression of FAS and that led to the activation of caspase 9 and caspase 3 [54]. This study further suggested that in addition to FAS, p53 can also induce expression of the proapoptotic gene *BAX* [55,56]. Since we also observe elevated levels of p53 upon treatment with DFH and note an upregulation of BAD and activation of caspases, a similar mechanism might be occurring in DFH treated cells. However, the effect of DFH on FAS remains to be explored.

The observed reduction in the expression levels of Ku70 and Ku80 proteins when treated with DFH is also of interest. Since these proteins are involved in the DNA double-strand break repair, downregulation of Ku70 and Ku80 is expected to promote apoptosis as NHEJ cannot take place [57–60]. A comparable reduction in the level of Ku70 was reported when justicidine was treated with human colorectal cancer cells [61]. This study and other studies have also suggested that Ku70 can inhibit the translocation of proapoptotic protein BAX from cytosol to mitochondria by sequestering BAX [61,62]

4.3. *Proposed mechanism of apoptosis induced by DFH*

For the first time, we show that a spirohydantoin derivative induces growth inhibition and apoptosis in leukemic cells. Mechanistically our data supports the induction of apoptosis by activation of the mitochondrial pathway (Fig. 9). In summary, the fluorinated spirohydantoin, DFH induces DNA damage causing downregulation in the expression of anti-apoptotic proteins like BCL2. Downregulation of BCL2 induces the activation of caspase 9, most likely through the mitochondrial release of cytochrome c. The activated caspase 9 in turn activates caspase 3 to cleave PARP. The cleavage of PARP hampers its ability to carry out poly-ADP-ribosylation of various proteins involved in DNA repair like Ku70 and Ku80 causing the failure of repair of damaged DNA. This will lead to degradation of cellular DNA. Simultaneously, activated caspase 3 also activates nucleases, which will also cause the degradation of the nuclear DNA leading to apoptosis (Fig. 9). Further as shown, DFH induced DNA damage can lead to elevated expression of p53, which could trigger the expression of proapoptotic proteins like BAD, BAX, etc. (Fig. 9). More research is needed to be done to understand the mechanism of cell proliferation defect and cell cycle arrest induced by DFH.

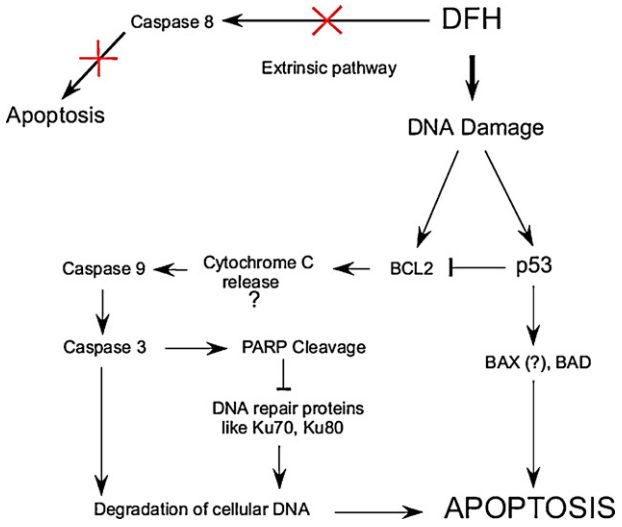

Fig. 9 – Proposed model for the mechanism of DFH induced cytotoxicity through apoptosis. DFH treatment of cells resulted in the induction of DNA damage, which could induce apoptosis through one of the following pathways for exhibiting the cytotoxic effect. First, the DNA damage induced by DFH could lead to the downregulation of BCL2. Downregulation of BCL2 probably leads to loss of mitochondrial membrane permeability due to cytochrome c release which further leads to the activation of the initiator caspase 9. This results in the activation of the apoptotic protein cascade wherein caspase 3 gets cleaved and activated which can further either induce PARP cleavage or cleave the inhibitor of the caspase-activated DNase which finally results in fragmentation and degradation of the cellular DNA. PARP cleavage may also result in the downregulation of the DNA double-strand break repair proteins like Ku70/80 which further supports the nuclear DNA degradation and finally apoptosis. The reduced expression of BCL2 could also be due to the elevated levels of p53 following DNA damage induced by DFH. The elevated levels of p53 can also modulate the expression of the proapoptotic/antiapoptotic proteins. The resulting increased levels of the proapoptotic proteins like BAD and possibly BAX can directly result in apoptosis.

for the expression of BCL2, BAD (A), caspase 8 (B), PARP (C), procaspase 3 and caspase 9 (D), p53 (E) and Ku70, Ku80 (F) with specific primary antibodies and secondary antibody. The α-tubulin was used as an internal loading control. In all panels, "0" is DMSO control; "24", "48", "72" are cells harvested after 24, 48 and 72 h of DFH treatment, respectively. See figure legend 4 for other details. For each protein, respective intensity of bands were quantified and presented as histogram.

Thus, our results imply that DFH and DCH possibly act as chemopreventive agents inducing inhibition of the growth of leukemia cells and induction of apoptosis. Our studies suggest that in addition to its use in other avenues of treatment of human diseases, hydantoin derivatives may be developed as chemotherapeutic agents against leukemia. However, more in depth studies both at *in vitro* and *in vivo* level are required for strengthening our current findings.

Conflict of interest statement

Authors disclose that there is no conflict of interest.

Acknowledgements

We thank Dr. Kumaravel Somasundaram, Ms. Vijayalakshmi Kari, Dr. Shahabuddin M.S., Dr. Binu Tharakan and members of the SCR laboratory for discussions and help. We thank Dr. Omana Joy and Vamsi for help in FACS analysis. This work was supported by Lady Tata Memorial Trust international award for leukemia research, and IISc start up grant for SCR. We also thank Dr. Raghavan Varadarajan for financial assistance. KSR acknowledges support from UGC-SAP and DST-FIST programmes. KCV is supported by DBT postdoctoral fellowship from DBT, India.

Appendix A. Supplementary data

Supplementary data associated with this article can be found, in the online version, at doi:10.1016/j.bcp.2008.10.018.

REFERENCES

[1] Nambiar M, Kari V, Raghavan SC. Chromosomal translocations in cancer. BBA Rev Cancer 2008;1786:139–52.
[2] Nickoloff JA, De Haro LP, Wray J, Hromas R. Mechanisms of leukemia translocations. Curr Opin Hematol 2008;15:338–45.
[3] Aplan PD. Causes of oncogenic chromosomal translocation. Trends Genet 2005;22:46–55.
[4] Rowley JD. Chromosome translocations: dangerous liaisons revisited. Nat Rev Cancer 2001;1:245–50.
[5] Raghavan SC, Lieber MR. DNA structures at chromosomal translocation sites. Bioessays 2006;28:480–94.
[6] Raghavan SC, Swanson PC, Wu X, Hsieh CL, Lieber MR. A non-B-DNA structure at the Bcl-2 major breakpoint region is cleaved by the RAG complex. Nature 2004;428:88–93.
[7] Raghavan SC, Kirsch IR, Lieber MR. Analysis of the V(D)J recombination efficiency at lymphoid chromosomal translocation breakpoints. J Biol Chem 2001;276:29126–33.
[8] Marculescu R, Le T, Simon P, Jaeger U, Nadel B. V(D)J-mediated translocations in lymphoid neoplasms: a functional assessment of genomic instability by cryptic sites. J Exp Med 2002;195:85–98.
[9] Lieber MR, Yu K, Raghavan SC. Roles of nonhomologous DNA end joining, V(D)J recombination, and class switch recombination in chromosomal translocations. DNA Repair (Amst) 2006;5:1234–45.
[10] Dorsett Y, McBride KM, Jankovic M, Gazumyan A, Thai TH, Robbiani DF, et al. MicroRNA-155 suppresses activation-induced cytidine deaminase-mediated Myc-Igh translocation. Immunity 2008;28:630–8.
[11] Yu K, Roy D, Bayramyan M, Haworth IS, Lieber MR. Fine-structure analysis of activation-induced deaminase accessibility to class switch region R loops. Mol Cell Biol 2005;25:1730–6.
[12] Okazaki IM, Kotani A, Honjo T. Role of AID in tumorigenesis. Adv Immunol 2007;94:245–73.
[13] Canadian Cancer Society–National Cancer Institute of Canada. Canadian Cancer Statistics Toronto; 2005.
[14] Nowell PC, Hungerford DA. A minute chromosome in human chronic granulocytic leukemia. Science 1960;132:1497.
[15] Moen MD, McKeage K, Plosker GL, Siddiqui MA. Imatinib: a review of its use in chronic myeloid leukaemia. Drugs 2007;67:299–320.
[16] Robert J, Jarry C. Multidrug resistance reversal agents. J Med Chem 2003;46:4805–17.
[17] Huang C, Yang S, Ge R, Sun H, Shen F, Wang Y. ZNF23 induces apoptosis in human ovarian cancer cells. Cancer Lett 2008;266:135–43.
[18] Kohn EA, Yoo CJ, Eastman A. The protein kinase C inhibitor Gö6976 is a potent inhibitor of DNA damage-induced S and G2 cell cycle checkpoints. Cancer Res 2003;63:31–5.
[19] Tang DG, Porter AT. Target to apoptosis: a hopeful weapon for prostate cancer. Prostate 1997;32:284–93.
[20] Buolamwini JK. Cell cycle molecular targets in novel anticancer drug discovery. Curr Pharm Des 2000;6:379–92.
[21] Williams DA, Lemke TL. Foye's principles of medicinal chemistry. Philadelphia: Lippincott Williams & Wilkins; 2002.
[22] Kleemann A, Engel J, Kutscher B, Reichert D. Pharmaceutical substances, synthesis, patents, applications; 2001.
[23] Fiallo M, Kozlowski H, Garnier-Suillerot A. Mitomycin antitumor compounds—Part 1. CD studies on their molecular structure. Eur J Pharm Sci 2001;12:487–94.
[24] Lee J, Kim J, Koh JS, Chung HH, Kim KH. Hydantoin derivatives as non-peptidic inhibitors of Ras farnesyl transferase. Bioorg Med Chem Lett 2006;16:1954–6.
[25] Rajic Z, Zorc B, Raic-Malic S, Ester K, Kralj M, Pavelic K, et al. Hydantoin derivatives of L- and D-amino acids: synthesis and evaluation of their antiviral and antitumoral activity. Molecules 2006;11:837–48.
[26] Carmi C, Cavazzoni A, Zuliani V, Lodola A, Bordi F, Plazzi PV, et al. 5-Benzylidene-hydantoins as new EGFR inhibitors with antiproliferative activity. Bioorg Med Chem Lett 2006;16:4021–5.
[27] Kirk KL. Selective fluorination in drug design and development: an overview of biochemical rationales. Curr Top Med Chem 2006;6:1447–56.
[28] Kirk KL. Fluorine in medicinal chemistry: recent therapeutic applications of fluorinated small molecules. J Fluorine Chem 2006;127:1013–29.
[29] Bégué J-P, Bonnet-Delpon D. Fluorine: an invaluable tool in medicinal chemistry. Actualite Chimique 2006;83–7.
[30] Mueller K, Faeh C, Diederich F. Fluorine in pharmaceuticals: looking beyond intuition. Science 2007;317:1881–6.
[31] Swinson J. Fully functional fluorine. Pharmachem 2007;4:38–41.
[32] Isanbor C, O'Hagan D. Fluorine in medicinal chemistry: a review of anti-cancer agents. J Fluorine Chem 2006;127:303–19.
[33] Dolzhenko AV, Dolzhenko AV, Chui WK. Advances in chemistry and biological activity of fluorinated 1,3,5-

triazines. In: Gardiner IV, editor. Fluorine chemistry research advances. New York: Nova Science Publishers Inc.; 2007. p. 105–42.
[34] Ananda Kumar CS, Benaka Prasad SB, Vinaya K, Chandrappa S, Thimmegowda NR, Ranganatha SR, et al. Synthesis and antiproliferative activity of substituted diazaspiro hydantoins: a structure–activity relationship study. Invest New Drugs, doi:10.1007/s10637-008-9150-3.
[35] Ananda Kumar CS, Kavitha CV, Vinaya K, Benaka Prasad SB, Thimmegowda NR, Chandrappa S, et al. Synthesis and in vitro cytotoxic evaluation of novel diazaspiro bicyclo hydantoin derivatives in human leukemia cells: a SAR study. Invest New Drugs, doi:10.1007/S10637-008-9179-3.
[36] Freimoser FM, Jakob CA, Aebi M, Tuor U. The MTT [3-(4,5-dimethylthiazol-2-yl)-2,5-diphenyltetrazolium bromide] assay is a fast and reliable method for colorimetric determination of fungal cell densities. Appl Environ Microbiol 1999;65:3727–9.
[37] Korzeniewski C, Callewaert DM. An enzyme-release assay for natural cytotoxicity. J Immunol Methods 1983;64:313–20.
[38] Singh NP, McCoy MT, Tice RR, Schneider EL. A simple technique for quantitation of low levels of DNA damage in individual cells. Exp Cell Res 1988;175:184–91.
[39] Ioannou YA, Chen FW. Quantitation of DNA fragmentation in apoptosis. Nucleic Acids Res 1996;24:992–3.
[40] Kaufmann SH, Desnoyers S, Ottaviano Y, Davidson NE, Poirier GG. Specific proteolytic cleavage of poly(ADP-ribose) polymerase: an early marker of chemotherapy-induced apoptosis. Cancer Res 1993;53:3976–85.
[41] Miranda CL, Stevens JF, Helmrich A, Henderson MC, Rodriguez RJ, Yang Y-H, et al. Antiproliferative and cytotoxic effects of prenylated flavonoids from hops (*Humulus lupulus*) in human cancer cell lines. Food Chem Toxicol 1999;37:271–85.
[42] Sakayama K, Mashima N, Kidani T, Miyazaki T, Yamamoto H, Masuno H. Effect of cortisol on cell proliferation and the expression of lipoprotein lipase and vascular endothelial growth factor in a human osteosarcoma cell line. Cancer Chemother Pharmacol 2008;61:471–9.
[43] Nowak SJ, Corces VG. Phosphorylation of histone H3: a balancing act between chromosome condensation and transcriptional activation. Trends Genet 2004;20:214–20.
[44] Anselmi C, Ettorre A, Andreassi M, Centini M, Neri P, Di Stefano AD. In vitro induction of apoptosis vs. necrosis by widely used preservatives: 2-phenoxyethanol, a mixture of isothiazolinones, imidazolidinyl urea and 1,2-pentanediol. Biochem Pharmacol 2002;63:437–53.
[45] Reed JC. Bcl-2-family proteins and hematologic malignancies:history and future prospects. Blood 2008;111:3322–30.
[46] Kelekar A, Thompson CB. Bcl-2-family proteins: the role of the BH3 domain in apoptosis. Trends Cell Biol 1998;8:324–30.
[47] Westphal S, Kalthoff H. Apoptosis: targets in pancreatic cancer. Mol Cancer 2003;2.
[48] Ahsan H, Reagan-Shaw S, Breur J, Ahmad N. Sanguinarine induces apoptosis of human pancreatic carcinoma AsPC-1 and BxPC-3 cells via modulations in Bcl-2 family proteins. Cancer Lett 2007;249:198–208.
[49] Thornberry NA. Caspases: key mediators of apoptosis. Chem Biol 1998;5:R97–103.
[50] Nicholson DW, Thornberry NA. Caspases: killer proteases. Trends Biochem Sci 1997;22:299–306.
[51] Kim JW, Won J, Sohn S, Joe CO. DNA-binding activity of the N-terminal cleavage product of poly(ADP-ribose) polymerase is required for UV mediated apoptosis. J Cell Sci 2000;113:955–61.
[52] Dong M, Nio Y, Yamasawa K, Toga T, Yue L, Harada T. p53 alteration is not an independent prognostic indicator, but affects the efficacy of adjuvant chemotherapy in human pancreatic cancer. J Surg Oncol 2003;82:111–20.
[53] Polyak K, Waldman T, He TC, Kinzler KW, Vogelstein B. Genetic determinants of p53-induced apoptosis and growth arrest. Genes Dev 1996;10:1945–52.
[54] Rho JK, Choi YJ, Ryoo B-Y, Na II, Yang SH, Kim CH, et al. p53 enhances gefitinib-induced growth inhibition and apoptosis by regulation of Fas in non-small cell lung cancer. Cancer Res 2007;67:1163–9.
[55] Miyahsita T, Reed JC. Tumor suppressor p53 is a direct transcriptional activator of the human bax gene. Cell 1995;80:293–9.
[56] Friesen C, Herr I, Krammer PH, Debatin KM. Involvement of the CD95 (APO-1/FAS) receptor/ligand system in drug-induced apoptosis in leukemia cells. Nat Med 1996;2:574–7.
[57] Hefferin ML, Tomkinson AE. Mechanism of DNA double-strand break repair by non-homologous end joining. DNA Repair (Amst) 2005;4:639–48.
[58] Lieber MR. The mechanism of human nonhomologous DNA end joining. J Biol Chem 2008;283:1–5.
[59] Chiruvella KK, Sankaran SK, Singh M, Nambiar M, Raghavan SC. Mechanism of DNA double-strand break repair. ICFAI J Biotechnol 2007;1:7–22.
[60] Gama V, Yoshida T, Gomez JA, Basile DP, Mayo LD, Haas AL, et al. Involvement of the ubiquitin pathway in decreasing Ku70 levels in response to drug-induced apoptosis. Exp Cell Res 2006;312:488–99.
[61] Lee J-C, Lee C-H, Su C-L, Huang C-W, Liu H-S, Lin C-N, et al. Justicidin A decreases the level of cytosolic Ku70 leading to apoptosis in human colorectal cancer cells. Carcinogenesis 2005;26:1716–30.
[62] Cohen HY, Lavu S, Bitterman KJ, Hekking B, Imahiyerobo TA, Miller C, et al. Acetylation of the C terminus of Ku 70 by CBP and PCAF controls Bax-mediated apoptosis. Mol Cell 2004;13:627–38.